# INTAKE CAPABILITY IMPROVEMENTS IN RAMJET-TYPE PROPULSION SYSTEM

**A.CHEVAGIN**
**Central Aerohydrodynamic Institute (TsAGI), Russia**
*Chevagin@tsagi.ru*

## Abstract

*The high speed (HS) ramjet intake capability influence upon the propulsion thrust and economic characteristics are discussed in the paper. The results of experimental study of intake start conditions that define the ramjet intake capability are presented. A possibility of the start throat area reduction in comparison with Kantrowitz limit is shown. The allowable intake internal contraction ratio is obtained. The computation methodology of intake start throat area is presented. The computational results are compared to the experimental ones.*

## Introduction

The given paper considers two issues that define the ramjet efficiency under high supersonic flight velocities. The first one refers to the influence of intake capability on the operation process parameters and the propulsion characteristics. The second issue covers the flow start conditions in intake that limits the allowable flow intake capability. The development and the justification are highlighted of ways to reduce the inlet throat area that is demanded to autonomous start with-out application of special means to control and with-out the boundary layer suction.

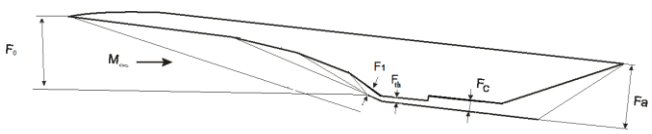


Fig.1. Ramjet propulsion flowpath sketch

The fixed nonadjustable HS ramjet arrangement is under consideration (Fig.1).

According to the available experimental and computation data the ramjet specific impulse is sharply dropping as the Mach flight number is ever growing (Fig.2). Besides the main cause i.e. the reduction of the relative heat-supply inside the combustor as far as the flight velocities are ever growing, the problem is often worsening due to the absence of the geometry control and the boundary layer suction. The application of nonadjustable air intakes, the throat area which of is chosen based on the known flow start conditions under initial M number to start flow ($M_{start}$), may fail to provide the necessary throat area values (i.e. the intake capability) at acceleration and cruise under M numbers $M_\infty > M_{start}$.

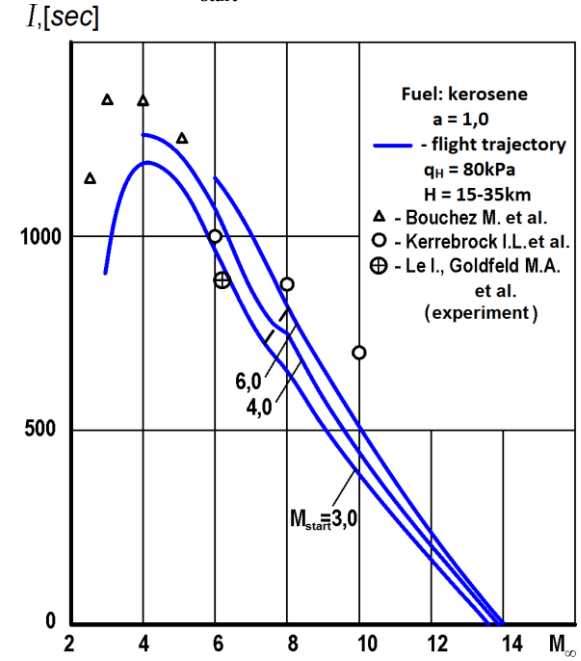


Fig.2. Computation and experimental specific impulse values for the nonadjustable HS ramjet

Two ways are possible to be proposed to enhance the ramjet specific impulse. The first

one assumes to reduce the velocities range and to approximate the M numbers of ramjet operation start to the M number of cruise flight. In this case the throat area $F_{th}$ may be reduced accordingly to the growing $M_{start}$.
The second way is to use the nonconventional techniques to enhance the inlet compression, expressed by contraction ratio, due to reduction of inlet throat area that is allowable to provide the start vs the known data and approaches.
These techniques are presented and justified in the second section of this paper.

## 1 Intake capability influence upon the HS ramjet properties

The flowpath geometry of the isolated HS ramjet that was tested in TsAGI T-131 wind tunnel is considered (Fig.1). The intake designed Mach number is M=6, the mass flow ratio is f=1. The relative throat area was varied in $\overline{F}_{th} = F_{th}/F_0 = 0.12 - 0.25$ range. The intake capability expressed by contraction ratio was $F_0/F_{th} = 1/\overline{F}_{th} = 4 - 8.33$. The relative combustor area is $F_c/F_{th} = 1.37$, the nozzle area is $F_a/F_0 = 1.5$. The thrust and specific impulse are calculated at Mach number M=6, the angle of attack is $\alpha = 0$ and the altitude is H=30km. The fuel used is kerosene. The calculation is performed based on the quasi-one-dimensional flow model in combustor and nozzle (E.A. Mesheryakov, TsAGI, 2005). The initial intake throat flow parameters are calculated by the methodology presented in Ref. [1].

Calculated Mach, pressure and temperature in throat section are given in Fig.3. As far as the throat area is reducing it is possible to observe the M number $M_{th}$ monotonic reduction accompanied by the simultaneous growth of relative pressure $P_{th}/P_\infty$ and temperature $T_{th}/T_\infty$. The distributions of relative pressure $P_{th}/P_\infty$ and the M numbers along the combustor length are presented for three throat areas values (see Fig.4). The data presented indicate that the combustor operates in ramjet regime. The combustion takes place in a subsonic flow and the pre-flame pressure wave emerges (pseudo-shock) that expands upstream from the fuel supply point up to the intake throat included.

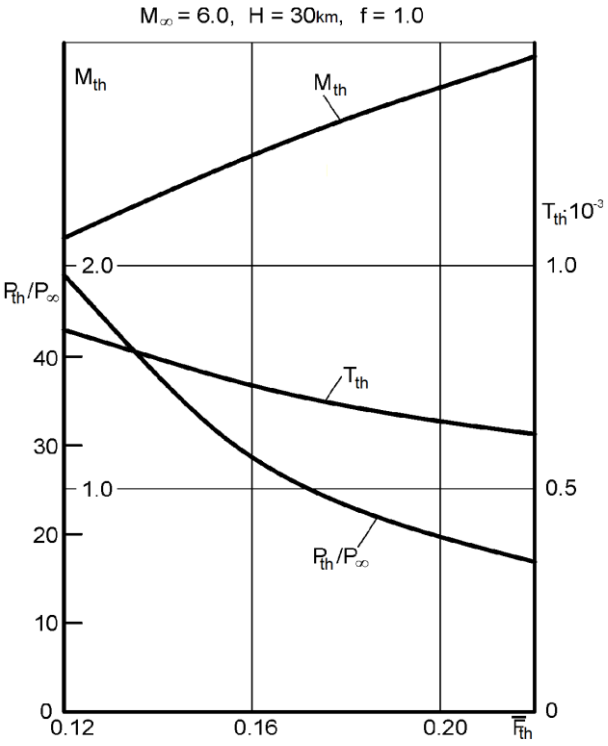


Fig.3. Mach number $M_{th}$ , the relative pressure $P_{th}/P_\infty$ and temperature in inlet $T_{th}$ vs the relative throat area

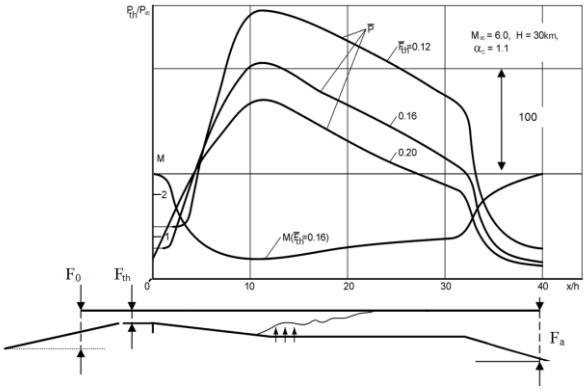


Fig. 4. The pressure and Mach distribution behavior along the ramjet flowpath vs the relative intake throat area

The flowpath pressure level is rising as the $\overline{F}_{th}$ area is ever reducing. The pressure growth is the main reason of evident growth of specific impulse I and of the thrust coefficient $C_t$, (see Fig.5). Besides, two factors more contribute into enhancing the ramjet characteristics as far as the throat area is reducing. First of all, when $\overline{F}_{th}$ is reducing the Mach number $M_{th}$ is

dropping at the combustor input and hence the total pressure losses are reduced when the heat is being supplied. Secondly, under the fixed nozzle area $F_{a,}$ when $\overline{F}_{th}$ is reducing the relative area flow expansion $F_a/F_{th}$ is growing and herewith the jet output impulse is growing as well.

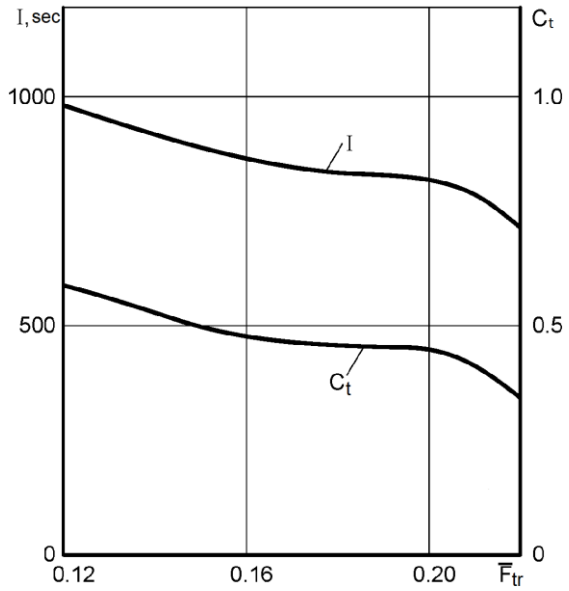


Fig.5. The HS ramjet specific impulse and thrust coefficient vs the relative inlet throat area

The Fig. 5 shows that the intake contraction ratio is an important way to enhance the HS ramjet characteristics. Therefore the requirement to minimize the relative throat area is one of the basic requirements to the propulsion flowpath geometry. But the $\overline{F}_{th}$ that is being implemented practically is bounded below value by the condition of creation of a internal supersonic flow that is known as the intake start. Because of these reasons it has become urgent to investigate the start process under high velocities in order to develop such aerodynamic duct shapes that would be able to provide the start under less throat area values that are practically being used currently.

## 2 Intake start

### 2.1 Problem status and research objective

The condition of start under supersonic flight velocities for the first time was formulated for stand-alone internal compression intake as "deglutition" of normal shock wave that is formed in front of the entry plane (Kantrowitz, [2, 3]). Later it was disseminated upon the inlet with the central body [4, 5]. For the inlet with central body from the conservation equations at input and at throat sections it was obtained:

$$\frac{F_{th}}{F_1} = \frac{q(\lambda_1)\cdot k}{q(\lambda_{th}=1)\cdot \nu_{\text{normal shock}}} = q\left(\frac{1}{\lambda_1}\right)\cdot k\,, \qquad (1)$$

where $q(\lambda)$ is a gas-dynamic function

$$q(\lambda) = \left(\frac{\kappa+1}{2}\right)^{\frac{1}{\kappa-1}} \lambda\left(1-\frac{\kappa-1}{\kappa+1}\lambda^2\right)^{\frac{1}{\kappa-1}} = \frac{\left(\frac{\kappa+1}{2}\right)^{\frac{\kappa+1}{2(\kappa-1)}} M}{\left(1+\frac{\kappa-1}{2}M^2\right)^{\frac{\kappa+1}{2(\kappa-1)}}}$$

$\lambda$ is a reduced velocity; $\nu_{\text{normal shock}}$ is a normal shock pressure recovery coefficient and $k = 1.03 \div 1.08$ is a boundary layer effect correction coefficient. In number of cases the computation results according (1) agree with the available experimental data at inlet entry Mach numbers $M_1 < 2.5\ldots3$ [2-8]. As an example it is possible to see the comparison in Figure 6 where the $F_1/F_{th}$ intake capability values of different inlets types are compared to the Kantrowitz start limit (the inverse value of dependence (1) is shown in the figure).

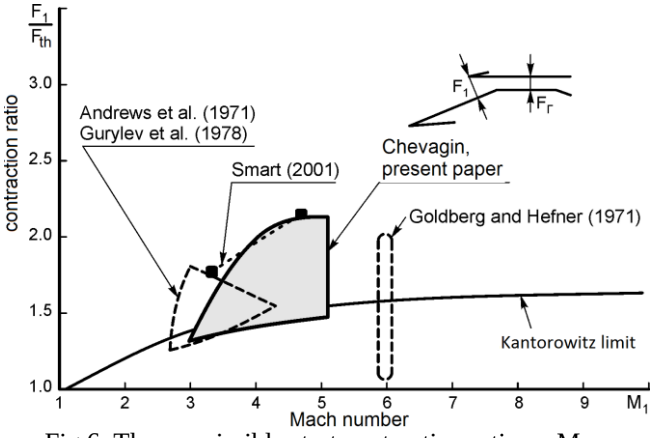


Fig.6. The permissible start contraction ratio vs $M_1$ number at the inlet input

When the flight velocities are getting higher ($M_1 > 3$) the flow structure at the inlet entry before start is getting more complicated. There is a developed separation on the central body in front of entry (Fig.7). Instead of the normal shock [2] the oblique shock wave

emerges that propagates from the separation zone outset up to cowl lip [6]. For such cases the start is considered as a complete one if the separation zone is pushed downstream and is fixed at the central body rapture line and the design shock wave system is being settled at the inlet entry.

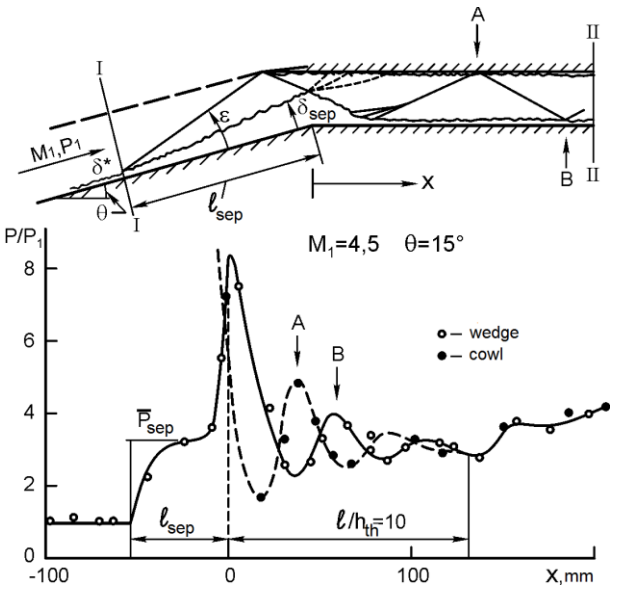


Fig. 7. The flow pattern and the pressure distribution at the inlet entry before start

The analysis of available test results and feasible flow patterns with separation zone that are realized before the start allows highlighting two peculiarities [6… 8]. The first one is that permissible throat areas $F_{th}/F_1$ as a rule are at the level of and higher than the dependence (1). Therefore this dependence is used in practical applications notwithstanding that the physical flow model used for the formula (1) not always corresponds to the actual flow pattern before the start. Such an approach is applied in the given paper for comparative analysis of the start conditions for conventional HS inlets.

The second peculiarity (that is the main one to justify the results presented below) is that under high Mach $M_1$ the flow velocity in throat immediately before the start is getting a supersonic one ($M_{th} > 1$) in spite of large separation at entry plane. This experimental phenomenon is used in the given paper to develop the ways to reduce the starting throat area (up to 35%) as compared to the dependence (1) due to creating the additional inner compression in convergent section of the intake.

All the said above defines the objectives of this paper:

- The study of mechanism and conditions of flow start in inlet with the considerable inner contraction ratio up to $F_1/F_{th} \sim 2.2$ (for comparison, the Kantrowitz limit is $F_1/F_{th} < 1.6$);
- The development of the rational aerodynamic shapes of intake with additional inner contraction as a way to reduce the start throat area under high velocities.

## 2.2 Intake model with additional inner contraction

The experiments were performed using the simplified mixed compression intake (Fig.8). The wedge has the contraction angle as $\theta = 10°$ or$15°$. The cowl angle is $\delta_c = 0$. The model is supplied with the optical glasses in lateral walls.

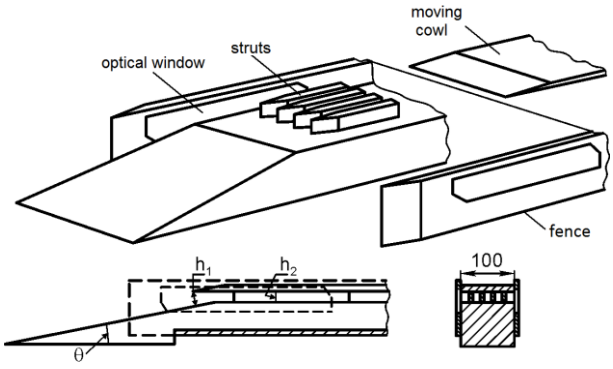


Fig. 8. The intake model with movable cowl to investigate the start conditions

Replaceable components were used inside the duct to create an additional inner flow compression. The additional compression was obtained by two ways: by the vertically mounted pylons for cross and longitudinal compression (see Fig.8, 9) and by the horizontal plates that were mounted serially on the cowl and the wedge, see Fig.10.

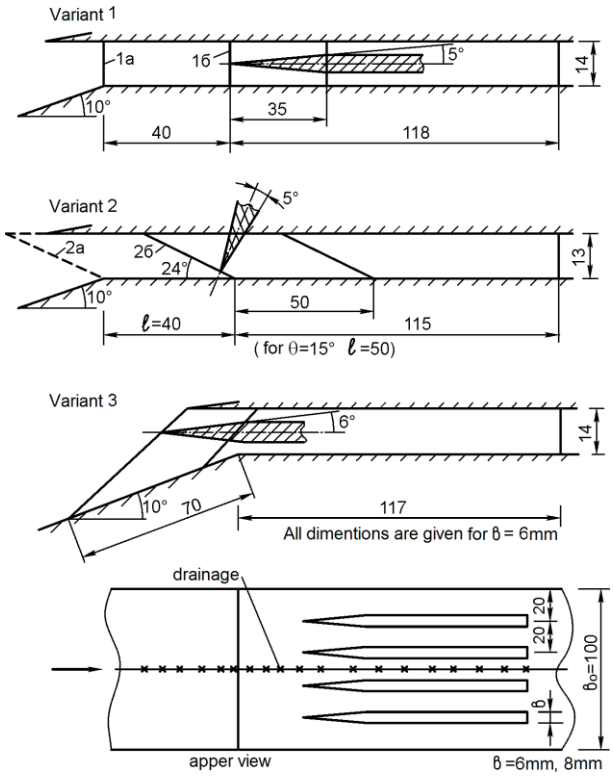


Fig. 9. The tested pylons versions for additional inner flow compression

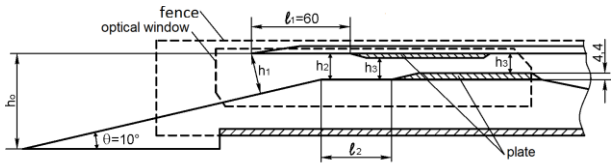


| Variant № | plate position | h₀, mm | h₂, mm | h₃, mm | h₃/h₂ | ℓ₁/h₂ | ℓ₂/h₂ |
|---|---|---|---|---|---|---|---|
| 1 | on cowl | 70 | 18,5 | 14,1 | 0,76 | 3,24 | – |
| 2 | on cowl | 65,5 | 14 | 9,6 | 0,686 | 4,28 | – |
| 3 | on wedge | 65,5 | 14 | 9,6 | 0,686 | – | 5,7 |
| 4 | on wedge | 70 | 18,5 | 14,1 | 0,76 | – | 3,21 |

Fig. 10. The tested plates versions for additional inner flow compression

The value of additional contraction in the both cases was as $F_3/F_2$ =0.6, 0.68 and 0.76 (here $F_3$=$F_{th}$). The shape and the locations of components that provided the inner contraction were varied (Fig.9,10).

The tests were performed using the "tantamount models method"[6], when the inlet flow is simulated from entry plane (section I-I in Fig.8) up to the reference section II-II (or III-III) in throat. This allows testing the models in available wind tunnels (WT) and obtaining the sufficiently high Mach numbers $M_1$ at entry that correspond to the flight Mach $M_\infty \le 10$ by reducing the wedge angle or angle of attack (α < 0). The given tests are performed in TsAGI SVS-2 WT at $M_1$ = 2.5…5 and $\mathrm{Re}_L = (7 \div 10)\cdot 10^6$. The following parameters were simulated: - the relative area $\overline{F}_{th} = \frac{F_{th}}{F_1} = \frac{h_{th}}{h_1}$, the angles $\theta - \delta_c$, the relative boundary layer displacement thickness $\frac{\delta^*}{h_1}$ and the area variation along the duct length $F(x)$ up to the reference section. The $\overline{F}_{th}$ relative throat area was being varied in by the cowl moving in longitudinal direction by electromotor in order to provide start/stall /restart of the intake. The inlet wedge could move along the height due to patch plates that were installed under its bottom and hereby it could change the physical height of throat and consequently the relative boundary layer thickness on the surface (at δ=const). The relative thickness of the boundary layer $\delta/h_1$ and $\delta^*/h_1$ were estimated following the methodology [9].

## 2.3 The experimental results of testing the start of inlet with inner contraction

Based on test results let's make some preliminary comments:

1. At the moment before the start the flow structure with large separation zone in front of entry is realized; the shock wave from separation crosses the cowl lip (Fig.8). The mass flow rate is maximal (the entering jet area is equal to the $F_1$ inlet entry area). The shock wave arriving to the cowl with the next ingress on its edge was one of the start conditions. The indefinitely small growth of M number or the moving of the cowl (increasing of relative throat area $\overline{F}_{th} = \frac{F_{th}}{F_1} = \frac{h_{th}}{h_1}$) resulted after this into the pushing of separation into duct, i.e. to the inlet start. It is to be mentioned that such a type of start made it possible to approve the assumption on the equality of relative areas $F_{th}/F_1$ just before the start and after it in calculations of start throat area below.

2. In Ref. [4…8] the $\overline{F}_{th}$ start values are obtained at comparatively low relative boundary layer displacement thickness $\delta^*/h_1 = 0.02 \div 0.04$. In the paper under consideration the intake start conditions are defined at higher values $\delta^*/h_1 \approx 0.1 \div 0.2$ that are typical for the actual hypersonic inlets. E.g. the inlet with $\theta - \delta_c = 10°$ angles ratio shows the considerable dependence of start area $\overline{F}_{th}$ upon $\delta^*/h_1$. (Fig.11). So, if $M_1 = 3.3$ and $\delta^*/h_1 = 0.02$ the start takes place at $\overline{F}_{th} = 0.6$, that is 13% less than the $\overline{F}_{th} = q\left(\frac{1}{\lambda_1}\right)$ dependence, then while the boundary layer thickness is increasing up to $\delta^*/h_1 \sim 0.2$ the required throat area is vice- versa increasing up to $\overline{F}_{th} = 0.79$ (by ~30%). The higher effect takes place when the flow turn angle is increasing up to $\theta - \delta_c \geq 15°$.

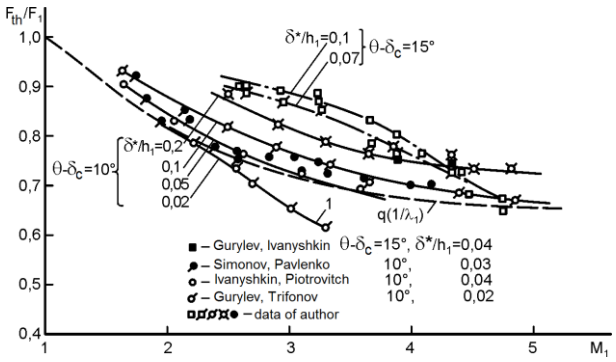


Fig. 11. The influence of the relative boundary layer displacement thickness $\delta^*/h_1$ and of the $\theta$-$\delta_c$ flow turn angle upon the relative start throat area

3. The $\overline{F}_{th}$ decrease that was observed at low $\delta^*/h_1 \approx 0.02 \div 0.1$ and $M_1 > 3$ values if comparing to $q\left(\frac{1}{\lambda_1}\right)$ dependence (see the curve line I in Fig.12 for $\theta - \delta_c = 10°$) in the given tests was not observed due to considerably higher relative displacement thickness $\delta^*/h_1$ ($2 \div 10$ times). Under such conditions the decrease of $\overline{F}_{th}$ values up to $\overline{F}_{th} = q\left(\frac{1}{\lambda_1}\right)$ level was observed only at higher M numbers $M_1 \geq 4.5 \div 4.8$.

The tests results presented below are obtained at $\delta^*/h_1 \approx 0.1$. It was found out experimentally that the $\overline{F}_{th}$ relative start throat area values of the inlet may by considerably reduced due to the additional flow contraction inside the duct. The concept of sequential (two-stepped) flow contraction is developed in this paper: firstly, the flow is compressed at the entry zone by the $\frac{F_2}{F_1} \sim q\left(\frac{1}{\lambda_1}\right)$ value (as for the conventional inlet) and then it is compressed directly in the throat region by a certain value of $\frac{F_3}{F_2} = f(M_1, \theta - \delta_c)$. So, when $M_1 = 4.5$, $\theta - \delta_c = 10°$ the allowable compression degree was $\frac{F_3}{F_2} = 0.68$. This reduced the total relative start throat area up to $\frac{F_{th}}{F_1} = \frac{F_3}{F_1} = \frac{F_2}{F_1} \times \frac{F_3}{F_2} = 0.675 \times 0.68 = 0.46$ as comparing to $\overline{F}_{th} = \frac{F_2}{F_1} = 0.675$ value for the conventional inlet without inner contraction (see Fig.12). The inner contraction effect obtained was the same both at the vertical pylons and the horizontal plates.

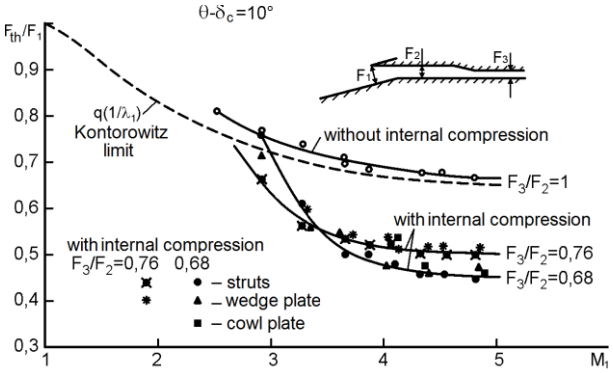


Fig. 12. The decrease of relative throat area of inlet start $F_{th}/F_1$ due to additional flow compression inside the duct

The similar effect was obtained when the flow turn angle was $\theta - \delta_c = 15°$ (Fig. 13).

This fact may be explained as follows. The experimental and computation estimations found out that the flow inside the throat region is supersonic just before the start. The average throat section Mach number may reach $M_2 = 2 \div 3$ in dependence of $M_1$ at entry and turn angle $\theta - \delta_c$ (Fig.14).

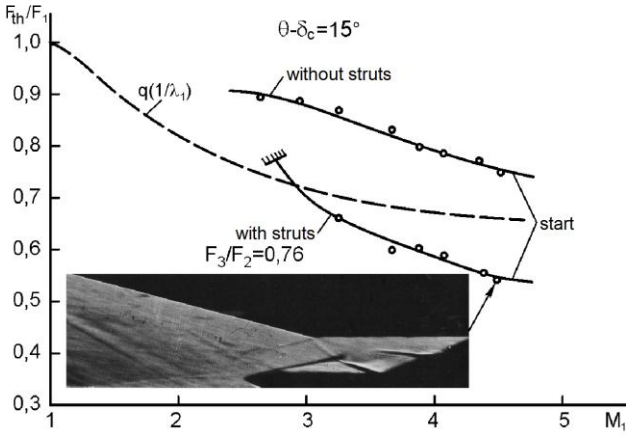


Fig. 13. The decrease of relative throat area of inlet start $F_{th}/F_1$ due to additional flow compression inside the duct

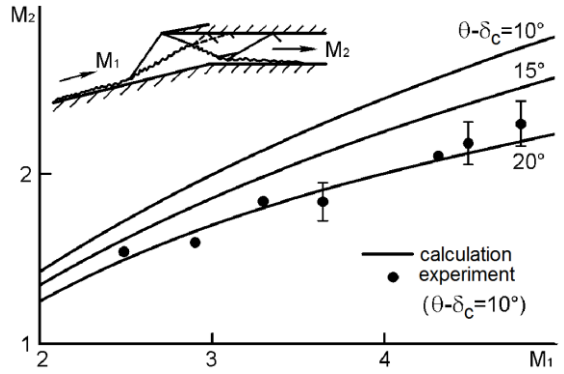


Fig. 14. The estimation of the averaged M number in inlet throat profile before start

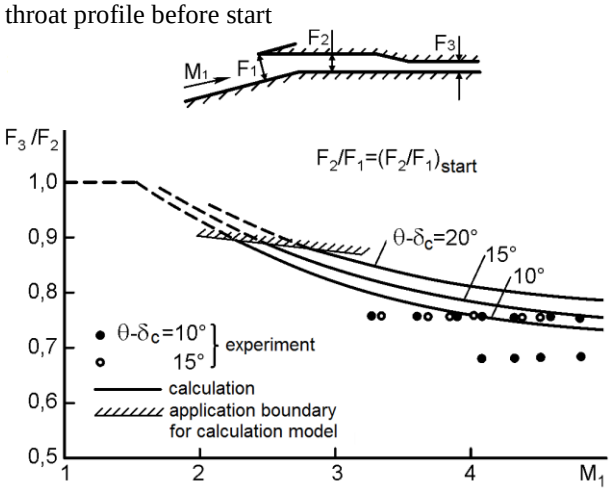


Fig. 15. Estimation of permissible degree of inlet inner contraction

In this case in the given supersonic flow field there may be realized such an additional internal geometrical compression that will not block the flow input in the entry part of the duct and will not change the $F_2/F_1$ value that is required for its start. The permissible area decrease under additional contraction depends upon the Mach number $M_1$ and the $\lambda_2$ reduced velocity before the place of internal contraction and may be estimated based on $\frac{F_3}{F_2} \approx q\left(\frac{1}{\lambda_2}\right)$ ratio (here, $\lambda_2$ value is calculated at the presence of separation in entry plane). The computation results using this formula are given in Fig.15 and 16. The slightly higher contraction was obtained in the experiment ($F_3/F_2$=0.68 и 0.76).

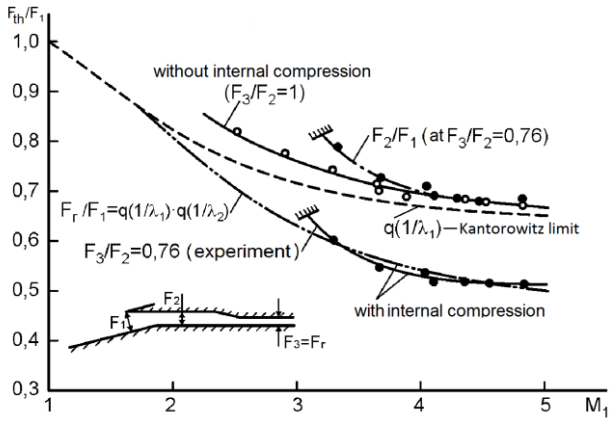


Fig. 16. The relative inlet start throat area with additional inner contraction

So, the value of $F_3/F_2$ inner contraction is to be chosen based on condition that provides the supersonic flow start in inner part even in the case when the separation presents in entry plane, i.e. when the external part of the inlet is unstarted. In this case the start of inlet with additional contraction ($F_3/F_2 < 1$) is carried out in the same way as if without the latter ($F_3/F_2 = 1$) under the same $F_2/F_1$ values.

Wherefrom it follows that the realization of the intake start is possible at sequential flow start: firstly, in inner part under the specified $\frac{F_3}{F_2} \sim q\left(\frac{1}{\lambda_2}\right)$ values and then in the entry part under $\frac{F_2}{F_1} \sim q\left(\frac{1}{\lambda_1}\right)$ values. The final $\overline{F}_{th}$ value will be as:

$$\frac{F_{\text{th}}}{F_1} = q\left(\frac{1}{\lambda_1}\right) q\left(\frac{1}{\lambda_2}\right) \qquad (2)$$

## 3 Calculation of intake start throat area

### 3.1 Basic correlations

Let's single out two calculated sections: I-I section in front of separation and the II-II section in throat zone (see Fig.7). Based on the equation of momentum conservation along $X$ axis we have:

$$(j_2 - j_1)_x = \int_{l_{\text{sep}}} P(x)\,dx + P_1 \frac{h_1}{\operatorname{tg}\varepsilon} \cdot \sin\theta, \qquad (3)$$

where $\theta$ is a wedge angle, $\varepsilon$ - wave shock angle away from separation, $\int_{l_{\text{sep}}} P(x)\,dx$ is a pressure force on the wedge in separation zone.

Approximately:

$$\int_{l_{\text{sep}}} P(x)\,dx = k\,P_{\text{sep}}\left(h_1\cos\theta - h_2 + \frac{h_1}{\operatorname{tg}\varepsilon}\cdot\sin\theta\right),$$

where $P_{\text{sep}}$ is a pressure in separation "plateau" zone, $k$ is an empirical coefficient that takes into account the actual pressure behavior $P(x)$ in separation (see Fig.8): $k = \dfrac{\int_{l_{\text{sep}}} P(x)\,dx}{P_{\text{sep}} \cdot l_{\text{sep}}}$.

From (3) it is easy to obtain:

$$z(\lambda_2) = z(\lambda_1)\cos\theta + \frac{2k_1\lambda_1\left[\dfrac{\sin\theta}{\operatorname{tg}\varepsilon}\left(1 - k\dfrac{P_{\text{sep}}}{P_1}\right) - k\dfrac{P_{\text{sep}}}{P_1}\cos\theta\right] + 2k_1\lambda_1 k\dfrac{P_{\text{sep}}}{P_1}}{(\kappa+1)\,M_1^2} \cdot \frac{h_2}{h_1} \qquad (4)$$

where $z(\lambda) = \lambda + \dfrac{1}{\lambda}$ is a gas-dynamic function,

$\lambda$ is a reduced velocity, $k_1 = \dfrac{1}{1 - \dfrac{\delta_1^*}{h_1}}$ is a coefficient that takes into account the initial boundary layer displacement thickness in I-I section.

Let the consumption equation be as:

$$\frac{1 - \dfrac{\delta_2^*}{h_2}}{1 - \dfrac{\delta_1^*}{h_1}} \cdot \frac{h_2}{h_1} \cdot \frac{1}{y(\lambda_1)} = \frac{1}{y(\lambda_2)} \cdot \frac{1}{P_2/P_1}, \qquad (5)$$

where

$$y(\lambda) = \left(\frac{\kappa+1}{2}\right)^{\frac{1}{\kappa-1}} \cdot \frac{\lambda}{1 - \dfrac{\kappa-1}{\kappa+1}\lambda^2},$$

$\dfrac{\delta_2^*}{h_2}$ is a relative displacement thickness in II-II section, wherefrom:

$$\frac{h_2}{h_1} = \frac{y(\lambda_1)}{y(\lambda_2)} \cdot \frac{1}{\overline{P}_2} \qquad (6)$$

(here $P_2$ is an averaged pressure in II-II section) in assumption that $\left(1 - \dfrac{\delta_2^*}{h_2}\right) \Big/ \left(1 - \dfrac{\delta_1^*}{h_1}\right) \to 1$.

The system that is composed of two equations (4) and (6) and four unknowns ($\lambda_2$, $P_{\text{sep}}/P_1$, $P_2/P_1$, $h_2/h_1$) is not closed. Let's define the additional relationships for $\overline{P}_{\text{sep}}$ and $\overline{P}_2$ values.

1. The comparison of the pressure obtained experimentally in separation "plateau" zone indicated the similarity to G. Petrov dependence under $M = 2 \div 5$, $\overline{T}_w = 1$ (here $\overline{T}_w$ is a temperature factor) [10, 11]:

$$\overline{P}_{\text{sep}} = 1 + 0.2\frac{\kappa M_1^2}{(M_1^2 - 1)^{0.25}} \qquad (7)$$

This dependence is used in further calculations.

2. The inlet throat pressure study found out that when approaching to the moment of start the $P_2$ averaged pressure level is decreasing constantly up to the determined threshold value after this the flow start is being realized. This $P_2$

threshold value, as the Fig.7 shows, is similar to the $P_{sep}$ separation "plateau" pressure. Therefore the equation below is assumed as an additional condition for start:

$$\frac{P_2}{P_1} = \frac{P_{отр.}}{P_1}. \qquad (8)$$

So, the system of equations (4) and (6) when meeting the conditions (7) and (8) becomes a closed one and is to be solved analytically.

It is easy to obtain:

$$\lambda_2^{\pm} = \frac{A \pm \sqrt{A^2 - 4\left(1 + k\,k_1 \frac{\kappa - 1}{\kappa + 1}\right)(1 - k\,k_1)}}{2\left(1 + k\,k_1 \frac{\kappa - 1}{\kappa + 1}\right)}, \qquad (9)$$

where

$$A = z(\lambda_1)\cos\theta + \frac{2k_1\lambda_1\left[\frac{\sin\theta}{\mathrm{tg}\,\varepsilon}\left(1 - k\,\bar{P}_{sep}\right) - k\,\bar{P}_{sep}\cos\theta\right] + 2k_1\lambda_1 k\frac{P_{sep}}{P_1}}{(\kappa+1)\mathrm{M}_1^2} \cdot \frac{h_2}{h_1}$$

$$\varepsilon = \arcsin\sqrt{\frac{7 + 3\mathrm{M}_1}{7\mathrm{M}_1^2}} \quad (\text{under } \kappa = 1.4).$$

From two values of $\lambda_2^{\pm}$ it should choose the solution with (+) before the square root, as the second value refers to the "subsonic" solution. $\lambda_2^{-} < 1$ does not correspond to factual flow pattern.

Finally:

$$\frac{h_2}{h_1} = \frac{y(\lambda_1)}{y(\lambda_2)} \cdot \frac{1}{\bar{P}_{sep}} = \frac{\lambda_1\left(1 - \frac{\kappa-1}{\kappa+1}\cdot\lambda_2^2\right)}{\lambda_2\left(1 - \frac{\kappa-1}{\kappa+1}\cdot\lambda_1^2\right)} \cdot \frac{1}{1 + 0.2\frac{\kappa\mathrm{M}_1^2}{(\mathrm{M}_1^2 - 1)^{0.25}}} \qquad (10)$$

where $\lambda_2$ is defined from (9) as $\lambda_2^{+}$.

## 3.2 Calculation vs experiment. The governing parameters influence

The results of calculating permissible start throat value $h_2/h_1$ under $\mathrm{M}_1 = 2 \div 5$, $\theta - \delta_c = 10°$ and $15°$, $\delta_1^*/h_1 = 0.09$ ($k_1 = 1.1$) are compared to the experimental ones (Fig.17). For the $P_{sep}$ value the $k$ correction factor is assumed to be 1 that approximately corresponds to experiment under $\mathrm{M}_1 > 2.5$, $\theta - \delta_c \le 15°$. The qualitative and quantitative similarity of calculation and experiment in mentioned conditions is evident.

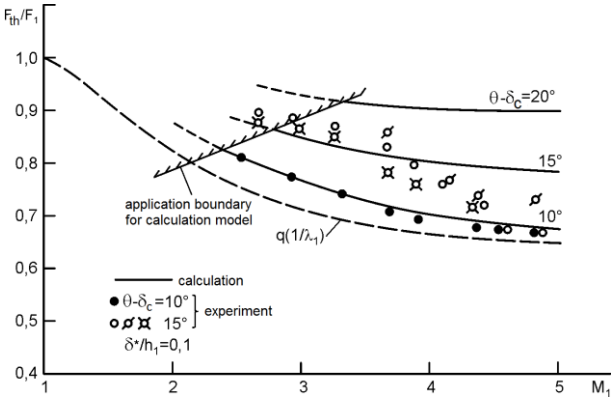


Fig. 17. The influence of inlet flow turn angle $\theta - \delta_c$ upon the relative start throat area

Strong dependence of start throat vs turn angle is observed. As $(\theta - \delta_c)$ is growing the $\lambda_2$ throat reduced velocity is increasing; the total pressure losses are growing. Both factors affect on $h_{th}/h_1$ start value growth. This result is necessary to be taken into consideration when designing the HS inlets.

Fig.18 shows the calculation results of $\frac{F_{th}}{F_1} = \frac{h_2}{h_1}$ start values under various values for relative boundary layer displacement thickness $\delta_1^*/h_1 = 0 \div 0.3$. The results of calculation qualitatively correspond to the available results of experiment.

These comparisons demonstrate the possibility to use the methodology presented to

estimate and analyze the influence of various parameters upon the start throat area.

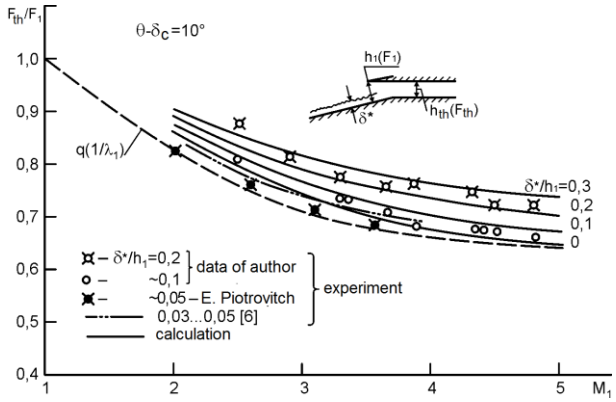


Fig. 18. The relative boundary layer displacement thickness influence upon the start throat area

It is evident from Fig.17 and 18 that the classic start limit (1) gives considerable errors in comparison with test for intake with central body under high values of $\theta - \delta_c = 15 \div 20°$, $\delta_1^* / h_1 \geq 0.1$, $M_1 > 2$.

## Conclusions

1. It is shown that the intake contraction ratio is an important way to enhance the high speed ramjet characteristics.

2. The methodology is developed for estimation of permissible start throat for intakes with central body taking into account the entry Mach numbers M1, the flow turn angles $\theta - \delta_c$, the areas distribution $F_i/F_1$ and boundary layer conditions.

3. It was found out by test and estimations the possibility of using an additional internal geometrical contraction in intake, witch gives considerable decrease of permissible throat area for intake start in comparison with classical Kantrowitz limit (up to 25…30%).

## References


[1] Penzin V.I. *On optimization of the flowpath shapes of dual-mode hypersonic ramjet (hypersonic bypass ramjet).* TsAGI Preprint №12, 1990.

[2] Kantrowitz A. *Theory and experiments on supersonic inlets and diffusers.* NASA Conference on Supersonic Aerodynamics. Ames Aeronautical Laboratory, 1946.

[3] Goldberg T. J., Hefner J. N., "Starting Phenomena for Hypersonic Inlets with Thick Turbulent Boundary Layers at Mach 6", NASA TN D-6280, 1971.

[4] Nikolaev A.V. *Flow at supersonic diffuser entrance part under boundary layer separation by leading wave.* «TsAGI Proceedings», v.I, №1, 1970.

[5] Gurylev V.G. *Flows with λ -type shocks at the supersonic flat inlets input.* «TsAGI Proceedings», v.III, №5, 1972.

[6] Gurylev V.G., Ivanyushkin A.K. Piotrovich E.V. *Experimental study of Re-numbers influence on inlets start under high supersonic flight velocities.* «TsAGI Proceedings», v. IV, №15, 1973.

[7] Simonov I.S., Stefanov S.A. *Flow at input and at throat zone of the supersonic flat inlet.* «TsAGI Proceedings», v.VI, №1, 1975.

[8] Smart M. *Advances on propulsion technology for high-speed aircraft.* RTO-AVT-VKI Lecture Series, 2007

[9] Garbuzov V.M., Kolina N.P., Pyatnova A.I. *Computation of coefficients of friction drag and heat transfer of the plate and the narrow cone that is streamlined by supersonic flow at presence of boundary layer turbulent stream.* TsAGI Transaction, iss.1881, 1977.

[10] Berlyand A.V., Glotov G.F., Ostras' V.N. *Research of supersonic flows with separation zones.* TsAGI R&S ID Review, №437, 1974.

[11] Pavlenko A.M. *On interaction problem of the incident oblique shock wave and the boundary layer on the plain surface with rapture.* «TsAGI Proceedings», v. XI, №3, 1980.


## Copyright Statement